Discovery of deep and shallow trap states from step structures of rutile TiO_2 vicinal surfaces by second harmonic and sum frequency generation spectroscopy

Hiroaki Takahashi, Ryosuke Watanabe, Yoshihiro Miyauchi, and Goro Mizutani[a)]
School of Materials Science, Japan Advanced Institute of Science and Technology, Asahidai, Nomi, Ishikawa 923-1292, Japan

(Received 27 January 2011; accepted 22 March 2011; published online 15 April 2011)

In this report, local electronic structures of steps and terraces on rutile TiO_2 single crystal faces were studied by second harmonic and sum frequency generation (SHG/SFG) spectroscopy. We attained selective measurement of the local electronic states of the step bunches formed on the vicinal (17 18 1) and (15 13 0) surfaces using a recently developed step-selective probing technique. The electronic structures of the flat (110)-(1×1) (the terrace face of the vicinal surfaces) and (011)-(2×1) surfaces were also discussed. The SHG/SFG spectra showed that step structures are mainly responsible for the formation of trap states, since significant resonances from the trap states were observed only from the vicinal surfaces. We detected deep hole trap (DHT) states and shallow electron trap (SET) states selectively from the step bunches on the vicinal surfaces. Detailed analysis of the SHG/SFG spectra showed that the DHT and SET states are more likely to be induced at the top edges of the step bunches than on their hillsides. Unlike the SET states, the DHT states were observed only at the step bunches parallel to [1 $\bar{1}$ 1] [equivalent to the step bunches formed on the (17 18 1) surface]. Photocatalytic activity for each TiO_2 sample was also measured through methylene blue photodegradation reactions and was found to follow the sequence: (110) < (17 18 1) < (15 13 0) < (011), indicating that steps along [0 0 1] are more reactive than steps along [1 $\bar{1}$ 1]. This result implies that the presence of the DHT states observed from the step bunches parallel to [1 $\bar{1}$ 1] did not effectively contribute to the methylene blue photodegradation reactions. © *2011 American Institute of Physics*. [doi:10.1063/1.3578178]

I. INTRODUCTION

Studies of TiO_2 photocatalytic reactions and their reactivity have attracted a lot of attention from researchers.[1–3] Second harmonic generation (SHG) is a useful and powerful tool to investigate the surface electronic properties of a TiO_2 photocatalyst due to its strong symmetric sensitivity.[4] Since SHG is permitted only at a point without inversion symmetry under the electric dipole approximation, SHG occurs only at TiO_2 surfaces or interfaces, namely, photocatalytic reaction fields. One can obtain the information on TiO_2 surface electronic states by using visible fundamental light, as the two-photon energies of visible light are resonant at valence-conduction interband electronic transitions of TiO_2. Especially for rutile TiO_2 (110), there have been a number of reports regarding wavelength dependence of SHG (SHG spectroscopy), rotational SHG measurements with respect to the surface normal, (time-resolved) pump–probe SHG measurements, and so on.[5–12]

In our recent report, we have applied the property of the symmetric sensitivity of SHG to vicinal surfaces of TiO_2 (110) with high step density.[13,14] Steps are generally known to have unique properties and strong influences on catalytic reactions as catalytic active sites,[15–18] and thus it is very important to investigate and clarify the electronic properties of TiO_2 step structures to understand TiO_2 photocatalytic reactions. We have recently developed a step-selective probing technique for vicinal TiO_2 surfaces and have proven that the SHG from (110) terraces can be forbidden by setting an incident light almost normal to the surface.[14] Moreover, we have also achieved indirect measurement of the local density of states (LDOS) corresponding to TiO_2 step atoms experimentally as a form of valence-conduction band joint density of states (JDOS) using SHG spectroscopy.[13] Ultraviolet photoemission spectroscopy (UPS) can also analyze surface band structures experimentally, but it cannot make a selective measurement of a particular structure on a surface, such as steps, as SHG spectroscopy does.[19] Thus SHG spectroscopy is a suitable method to inspect the electronic properties of TiO_2 surfaces, especially of TiO_2 step structures.

However, we had two problems left in our previous SHG spectroscopy:[13] (1) It was not confirmed whether the detected resonances were one-photon resonances (resonant at $\hbar\omega$) or two-photon resonances (resonant at $2\hbar\omega$), and (2) any spectroscopic information could not be obtained at SHG photon energies between 3.35 and 3.65 eV, where SHG intensity peaks should be located, as the light source of our optical parametric generator/amplifier (OPG/OPA) does not run at photon energies between 1.68 and 1.83 eV. In order to solve these problems, we introduced sum frequency generation (SFG) spectroscopy.[6] SFG is a nonlinear

a)Author to whom correspondence should be addressed. Electronic mail: mizutani@jaist.ac.jp.

optical process in which two inhomogeneous photons ($\hbar\omega_2$ and $\hbar\omega_3$) sum together to yield a SFG photon ($\hbar\omega_{SF} = \hbar\omega_2 + \hbar\omega_3$), while SHG is a nonlinear optical process in which two homogeneous photons ($\hbar\omega_1$) sum together to yield a SHG photon ($\hbar\omega_{SH} = 2\hbar\omega_1$). By introducing SFG spectroscopy, we successfully solved both the problems of the spectroscopic uncertainty (see the experimental section for details).

It is well-known that TiO_2 (011) possesses the highest photocatalytic activity of all the rutile single crystal faces, while TiO_2 (110) possesses the lowest photocatalytic activity.[20] High photocatalytic activity of TiO_2 (011) has triggered extensive investigation of its structures, adsorption properties, and electronic properties.[21–30] Originally, a one-fold O atom in the so-called titanyl (Ti = O) model proposed for a (011)-(2×1) reconstructed structure by Beck *et al*. was believed to be a key atom responsible for the high reactivity of the (011) face due to its unique properties.[21–24] However, after the discovery of the more stable model for the (011)-(2×1) structure, or the brookite (001)-like model, researchers' attractions have gradually moved from the previously suggested titanyl (Ti = O) model to this model, and the titanyl (Ti = O) model is now almost discarded.[26–30] The surface of the brookite (001)-like model displays rather inert properties toward adsorbed molecules.[29] One of the issues has been how to explain the high photocatalytic activity of the (011) surface using this recently proposed model. Therefore, more investigation and discussion are called for to understand the notable reactivity of the (011) surface. In order to contribute to this issue, it is very important and interesting to compare the electronic properties of TiO_2 (011) to those of TiO_2 (110) using the surface-sensitive probes, SHG and SFG.

In this study the electronic properties of steps and terraces on rutile TiO_2 single crystal faces are extensively investigated by SHG and SFG spectroscopy in the context of trap states and LDOS near band-gap regions. We selected two low-index surfaces, (110) and (011), and two high-index surfaces, (17 18 1) and (15 13 0), to evaluate the electronic properties of steps and terraces. Furthermore, their photocatalytic activity was estimated through methylene blue photodegradation reactions so that we can relate local electronic structures to photocatalytic activity.

TiO_2 (17 18 1) and (15 13 0) are vicinal surfaces of (110) and are off-oriented toward [0 1 1] and [1 $\bar{1}$ 0], producing steps parallel to [1 $\bar{1}$ 1] and [0 0 1] of high density, respectively. The steps parallel to these directions are believed to be thermodynamically stable on rutile TiO_2 (110).[31] By comparing SHG/SFG responses between the (17 18 1) and (15 13 0) surfaces, it is expected that we can see how the difference of their step types and structures affects their local electronic structures.

In this paper we focus on trap states produced at the steps and terraces on the above four kinds of sample surfaces. It is very important to look into the properties of trap states because they are immediately involved in TiO_2 photocatalytic reactions by increasing the probability of interfacial charge transfer.[32] It is well known that photoexcited electrons and holes are quickly trapped by various kinds of surface trap states, before being transferred to adsorbed molecules at the interface.[33–36] Trap states on TiO_2 surfaces are mainly classified into shallow trap states and deep trap states.

The majority of the shallow trap states have been reported to originate from Ti3d defect states associated with surface/subsurface oxygen vacancies[37–46] or titanium interstitials in the near-surface region[47–49] and behave as electron trap states. These shallow electron trap (SET) states play a key role in photocatalytic reactions in the presence of O_2 molecules because electron scavenging by O_2 molecules at Ti3d defect sites provides the pathway to produce well-known oxidizing agents, such as superoxide ($O_2^{\bullet-}$), hydrogen peroxide (H_2O_2), and singlet molecular oxygen ($^1O_2$),[3,32,50–52] as well as prevents the recombination of holes.[53–55] As a matter of fact, Sirisuk *et al*. suggested that the photocatalytic activity of TiO_2 nanoparticles tends to become higher with the increasing of the number of surface oxygen vacancies, hence the number of the electron trap states.[56] In addition to the SET states, shallow hole trap states are also very important because they have a high oxidation potential and can directly oxidize reacting molecules.[33] However, experimental information is still scarce due to the difficulty in their detection.

Deep trap states have been observed through photoluminescence (PL) from rutile TiO_2 surfaces and have been reported to act as hole trap states.[42,57–62] Potential candidates for their origin are lattice oxygen atoms located at the subsurface layer just below the Ti−OH groups [Ti−O$^\bullet$ − Ti−OH],[63–65] oxygen atoms in basic hydroxyl groups, such as bridging hydroxyl groups [Ti−O−Ti−O$^\bullet$],[59–61,64–67] triply coordinated lattice oxygen atoms [Ti$_2$ = O$^\bullet$ − Ti],[59–61] and dissociatively adsorbed oxygen molecules at surface titanium interstitials diffusing from the bulk.[65] The presence of the deep hole trap (DHT) states is important because it is believed to be associated with the production of surface-bound hydroxyl radicals (Ti−$^\bullet$OH),[33,68] one of the strongest oxidizing agents. For instance, based on the new model of oxygen photoevolution reactions proposed by Nakato *et al*.,[59–61] H_2O molecules attacking a surface trapped hole at a triply coordinated lattice oxygen atom can generate a [Ti−OOH HO−Ti] structure. Other groups suggested that this structure can finally give rise to $^\bullet$OH radicals.[3,69]

In this manner, the presence of shallow or deep trap states can have a large impact on TiO_2 photocatalytic reactions. Thus further investigation of the properties of these trap states is very important to understand TiO_2 photocatalytic reactions.

II. EXPERIMENTAL AND THEORETICAL METHOD

We purchased rutile TiO_2 (110), (011), (17 18 1), and (15 13 0) with a size of 10 × 10 × 0.5 mm^3 from K&R creation Co., Ltd. In addition to these four samples, we also prepared TiO_2 (6 7 1) and (13 9 0) vicinal surfaces in order to analyze SHG/SFG signals from step structures more in detail. The (6 7 1) and (13 9 0) samples are exactly the same ones as were used in our earlier study.[14] Miscut angles of the (6 7 1) and (13 9 0) surfaces are about 10°, while those of the (17 18 1) and (15 13 0) surfaces are about 4°. The (6 7 1) and (17 18 1) surfaces are off-oriented toward [0 1 1] from (110), and the (13 9 0) and (15 13 0) surfaces are off-oriented toward [1 $\bar{1}$ 0]

TABLE I. Information on the miscut for each TiO_2 vicinal surface.

Crystal faces	Off-oriented directions	Step edge directions	Miscut angles (°)
(671)	[0 1 1]	//[1 $\bar{1}$ 1]	10.9
(17 18 1)	[0 1 1]	//[1 $\bar{1}$ 1]	3.9
(13 9 0)	[1 $\bar{1}$ 0]	//[0 0 1]	10.3
(15 13 0)	[1 $\bar{1}$ 0]	//[0 0 1]	4.1

from (110). The information on these four high-index surfaces is summarized in Table I.

All the as-received specimens went through 10-min HF etching (5%), followed by annealing at 800 °C in an O_2 gas for 2 h. After the annealing, they were immersed into a HF aqueous solution (5%) for 5 min again and were washed in pure water. The samples used for photocatalytic activity measurement were dipped into a methylene blue aqueous solution (50 μM) immediately after the washing and were left in the solution for more than one day to adsorb methylene blue molecules on the sample surfaces sufficiently. It should be noted that all these treatments except for the annealing were conducted in a clean room of class 1000.

We performed contact atomic force microscopy (AFM) for the (110), (011), (17 18 1), and (15 13 0) surfaces in an ambient condition to confirm their surface structures. The tip kept applying ~1 nN of force onto the sample surfaces while scanning them. We also performed reflection high energy electron diffraction (RHEED) for the (011) surface in a high vacuum condition at 10^{-7}–10^{-8} Torr at room temperature to confirm surface reconstruction.

Photocatalytic activity for the (110), (011), (17 18 1), and (15 13 0) surfaces was evaluated through methylene blue photodegradation reactions. By measuring the transmittance of a methylene blue aqueous solution at a wavelength of the absorption peak (~660 nm), we can estimate changes in the concentration of methylene blue molecules caused by a TiO_2 photodegradation reaction. We put a sample sufficiently adsorbed with methylene blue molecules into an acrylic reaction cell with an inner volume of 10 × 10 × 30 mm^3 and poured 1 mL of a methylene blue aqueous solution (10 μM). The light from the Xe lamp traveled through a filter and a monochromator, and was modulated by a 1000 Hz chopper (Fig. 1). We measured the transmittance of the light passing through the reaction cell using a lock-in amplifier and a photodiode. The other Xe lamp described in Fig. 1 was used as a light source for UV excitation. This white light passed through a UV-D33S filter to generate UV light and entered the TiO_2 sample almost vertically. The spot size at the sample surfaces and the power density of the UV excitation light was ~1 cm and ~50 mW/cm^2, respectively. The optical configuration shown in Fig. 1 enabled us to photoexcite a sample and measure the transmittance without moving the reaction cell. We measured the transmittance of a methylene blue aqueous solution at 660 nm immediately after the UV irradiation onto a sample for 15 min. We repeated this cycle 12 times, and thus the total UV illumination time was 3 h. For each sample, we conducted the same measurement 3 times and averaged them out. We kept the temperature in the room at 23 ± 1 °C during the measurement.

The experimental setup for the SHG/SFG spectroscopy is shown in Fig. 2. The light source for the SHG spectroscopy was delivered by an OPG/OPA system driven by a frequency-tripled mode-locked Nd^{3+} : YAG laser (355 nm) running at a repetition rate of 10 Hz and at a pulse width of 30 ps. We define the photon energy of this light as $\hbar\omega_1$. The scanning range of SHG photon energy was $\hbar\omega_{SH} = 2\hbar\omega_1 = 2.45$ to 3.90 eV. Two fundamental beams for the SFG spectroscopy were delivered by the OPG/OPA system and the mode-locked Nd^{3+} : YAG laser (1064 nm). We define the photon energy of the former as $\hbar\omega_2$ and that of the latter as $\hbar\omega_3 = 1.17$ eV. The photon energy $\hbar\omega_2$ was varied from 1.43 to 2.74 eV so that the SFG light could be resonant at surface electronic states of TiO_2 just like the SHG light. Thus, the scanning range of the resultant SFG photon energy was $\hbar\omega_{SF} = \hbar\omega_2 + \hbar\omega_3 = 2.59$ to 3.90 eV. As mentioned earlier, SHG spectroscopy itself cannot cover the photon energy range between 3.35 and 3.65 eV due to the oscillating wavelength of our OPG/OPA system. However, by introducing SFG spectroscopy, the energy range of interest (2.45–3.90 eV) can be completely covered.

The combination between SHG and SFG spectroscopy also helps us with distinction between one-photon and two-photon resonances. When SHG spectra and SFG spectra are plotted as a function of SHG/SFG photon energy on a common horizontal axis $\hbar\omega_{SH} = \hbar\omega_{SF}$ (Fig. 8), a one-photon

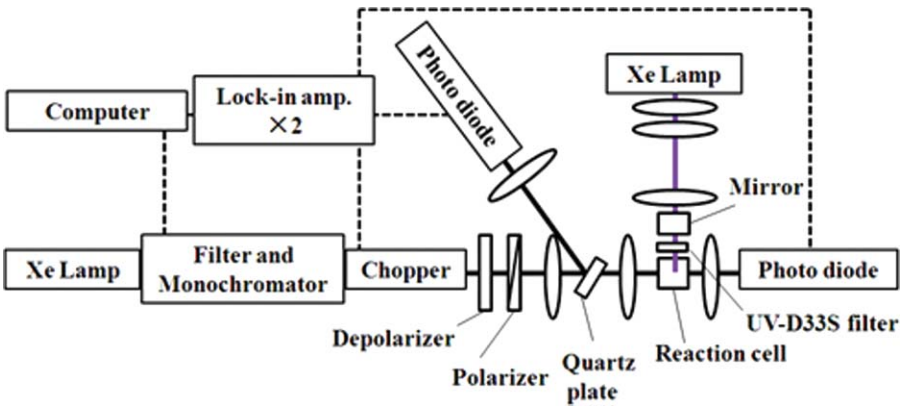

FIG. 1. Experimental setup for the TiO_2 photocatalytic activity measurement through methylene blue photodegradation reactions.

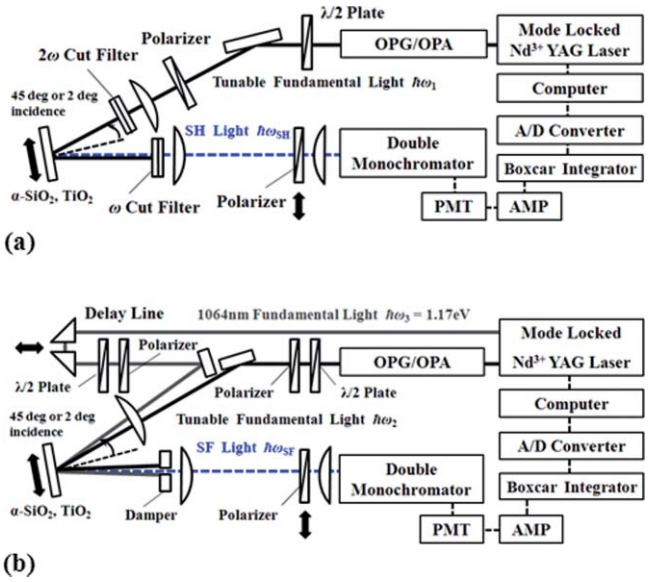

FIG. 2. Experimental setups for (a) the SHG spectroscopy and (b) the SFG spectroscopy. PMT and AMP represent a photomultiplier and an amplifier, respectively.

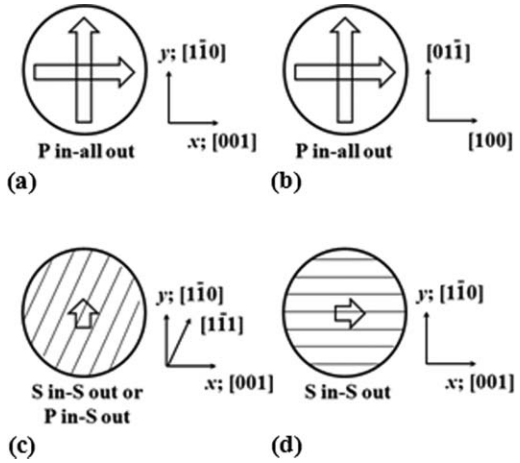

FIG. 3. Directions of incident beams (incident planes) in the SHG/SFG spectroscopy for (a) TiO_2 (110), (b) TiO_2 (011), (c) TiO_2 (6 7 1) and (17 18 1), and (d) TiO_2 (13 9 0) and (15 13 0). The arrows represent parallel components of incident wave vectors to a surface, $\vec{k}_{//}$. Step edges on the TiO_2 vicinal surfaces are indicated by solid lines.

resonance can be seen at different photon energies on the horizontal axis between the SHG spectra and the SFG spectra, as one-photon energies of SHG ($\hbar\omega_1$) and SFG ($\hbar\omega_2$) always satisfy $\hbar\omega_1 \neq \hbar\omega_2$ under the condition of $\hbar\omega_{SH} = \hbar\omega_{SF}$. Therefore, we can distinguish a one-photon resonance from a two-photon resonance by combining SFG spectroscopy with SHG spectroscopy.

The three fundamental beams ($\hbar\omega_1$, $\hbar\omega_2$, and $\hbar\omega_3$) were kept at an energy of less than 140 μJ/pulse. Their spot sizes at the sample surfaces were ~1 mm. We define the incident angle of light parallel to the surface normal (z axis) as 0°. Incident angles of all the three fundamental beams were set to ~45° for the (110) and (011) surfaces and were set to ~2° for the (6 7 1), (17 18 1), (13 9 0), and (15 13 0) vicinal surfaces. For the (110) and (011) surfaces, we fixed the polarizations of the three incident beams to P and observed the SHG/SFG beams without the limitation of their polarizations (P in-all out). For the (6 7 1) and (17 18 1) surfaces, we set the polarizations of the three incident beams to S or P and always fixed those of the SHG/SFG beams to S (S in-S out or P in-S out). For the (13 9 0) and (15 13 0) surfaces, the polarizations of all the beams were fixed to S (S in-S out). As shown in Fig. 3, directions of $\vec{k}_{//}$ on the sample surfaces were set to $\vec{k}_{//}$//[0 0 1] or $\vec{k}_{//}$//[1 $\bar{1}$ 0] for the (110) surface, $\vec{k}_{//}$//[1 0 0] or $\vec{k}_{//}$//[0 1 $\bar{1}$] for the (011) surface, $\vec{k}_{//}$//[1 $\bar{1}$ 0] for the (6 7 1) and (17 18 1) surfaces, and $\vec{k}_{//}$//[0 0 1] for the (13 9 0) and (15 13 0) surfaces, where $\vec{k}_{//}$ is a parallel component of the incident wave vector to a surface. In this study, the optical configuration described above for the high-index surfaces is referred to as "the terrace-forbidden and step-allowed optical configuration," and the configuration for the low-index surfaces is referred to as "the terrace-allowed optical configuration." The SHG/SFG intensity was calibrated by the signals from α-SiO_2 (0001) since the optical system itself has sensitivity variations with respect to the SHG/SFG photon energy.

We also calculated the LDOS for bulk, a terrace, and a step of the slab model with a TiO_2 (5 2 0) vicinal surface using density functional theory (DFT).[70] The step on this surface corresponds to the one on the (13 9 0) and (15 13 0) surfaces. We used the generalized gradient approximation (GGA) and the Perdew–Burke–Ernzerhof (PBE) functional to calculate the exchange correlation energy of electrons. The DFT calculation was conducted under a periodic boundary condition using the code of DMOL3 in Materials Studio (ACCELRYS, version 4.4).[70,71] The slab model was based on the result of the AFM measurement [Fig. 4(d)] and is explained in Sec. III D in detail.

III. RESULTS AND DISCUSSION

A. AFM and RHEED measurements

The AFM measurement was conducted for the TiO_2 (110), (011), (17 18 1), and (15 13 0) surfaces. The results are shown in Fig. 4. One can see that the (110) and (011) surfaces have very flat surfaces composed almost of terraces [Figs. 4(a) and 4(b)]. Steps on the (110) and (011) surfaces are almost uniformly distributed at an interval of ~200 and ~400 nm, respectively. The thicknesses of atomic monolayers for the (110) and (011) surfaces are known to be 0.325 nm[72] and 0.25 nm,[22] respectively. Thus the (110) surface is comprised of single-layer steps and flat terraces, while the (011) surface possesses triple-layer steps. Note that monoatomic steps were not observed on the (011) surface in this study as observed by other groups.[20,22]

For the (17 18 1) and (15 13 0) samples, multilayer step bunching[73,74] was observed from both of the vicinal surfaces as expected [Figs. 4(c) and 4(d)]. It is obvious that the step density of the (17 18 1) and (15 13 0) surfaces is much higher than that of the (110) and (011) surfaces. In Figs. 4(c) and 4(d), the edges of the step bunches on the (17 18 1) surface (designated as the step bunches // [1 $\bar{1}$ 1] in this study) are not straight and are rather wavy compared to those

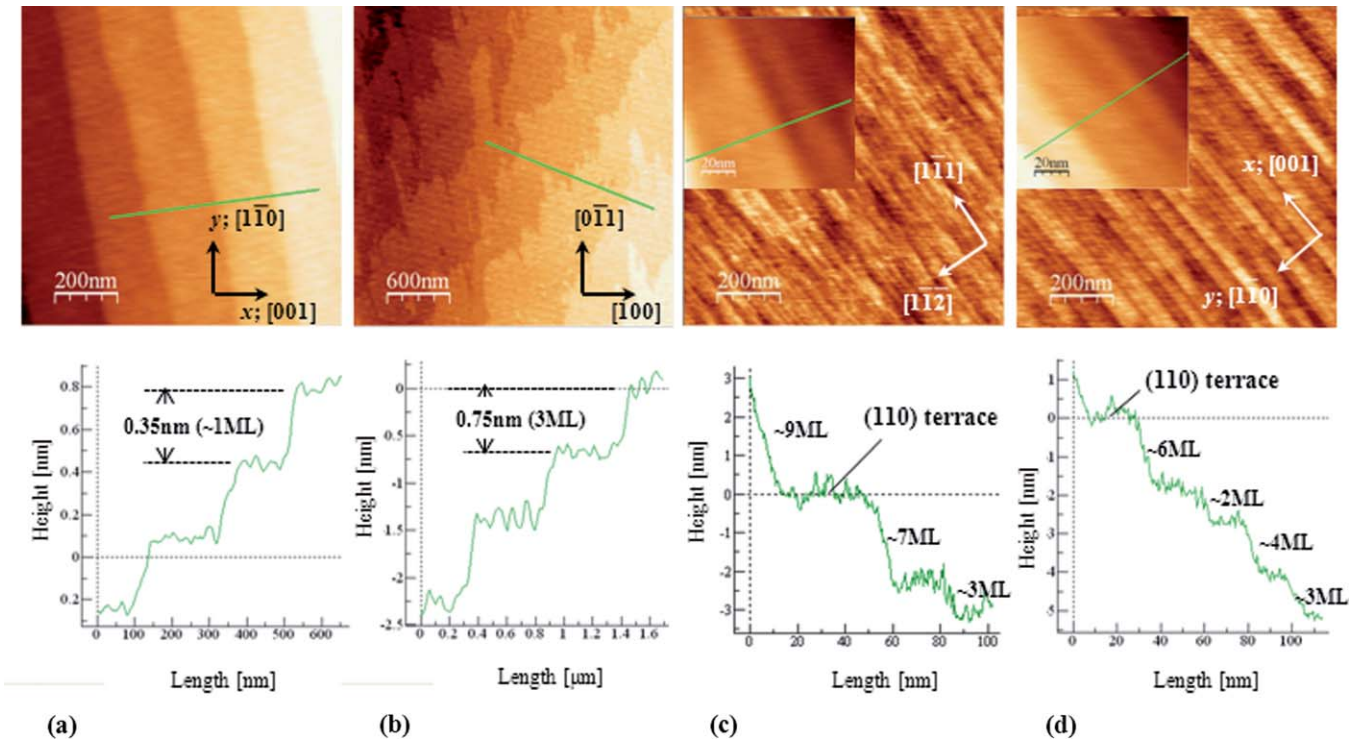

FIG. 4. Contact AFM images and their height profiles of (a) TiO_2 (110) (scanning area: $1.0 \times 1.0\ \mu m^2$), (b) TiO_2 (011) ($3.0 \times 3.0\ \mu m^2$), (c) TiO_2 (17 18 1) ($1.0 \times 1.0\ \mu m^2$), and (d) TiO_2 (15 13 0) ($1.0 \times 1.0\ \mu m^2$). Scanning areas of the insets in the images (c) and (d) are $100 \times 100\ nm^2$.

on the (15 13 0) surface (designated as the step bunches // [0 0 1] in this study). The step bunches // [0 0 1] look more in order. This result indicates that step bunches // [1 $\bar{1}$ 1] are not as thermodynamically stable as those // [0 0 1]. Based on the study reported by Diebold *et al.*,[31] we predicted the atomic structures at the top edges of the step bunches. The model of the top edge structures of the step bunches is depicted in Fig. 5. Unlike the structures around the top edges, it is more difficult to clearly picture the atomic structures on the hillsides of the step bunches due to their complicated structures. We believe that the hillside structures for the step bunches // [1 $\bar{1}$ 1] may be mainly composed of a (011) face, while those for the step bunches // [0 0 1] are probably composed of (100), (110), and $(1\ \bar{1}\ 0)$ faces.

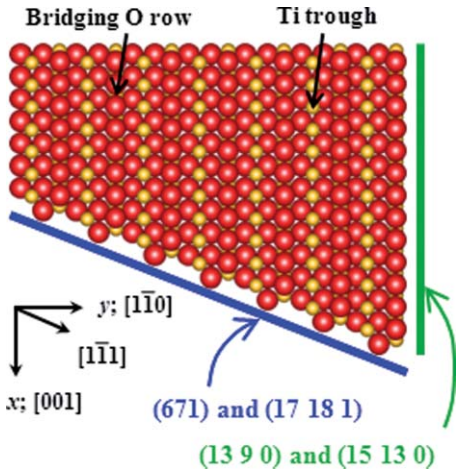

FIG. 5. Expected top edge structures of the step bunches corresponding to the (6 7 1), (17 18 1), (13 9 0), and (15 13 0) vicinal surfaces.

The average interval between these step bunches is estimated to be ~25 nm. Heights of the step bunches are about 1–3 nm (3–9 ML) for the (17 18 1) surface and are about 0.7–2 nm (2–6 ML) for the (15 13 0) surface. Note that the step bunches of the previously prepared (6 7 1) and (13 9 0) samples are also aligned at an interval of ~25 nm or a little more than that.[14] The difference between these 4° off-oriented and 10° off-oriented samples lies in the heights of their step bunches. That is, the average step heights for the (6 7 1) and (13 9 0) surfaces are ~2.5 ($= \tan 10^\circ / \tan 4^\circ$) times as large as those for the (17 18 1) and (15 13 0) surfaces if we assume that the intervals between the step bunches on the four vicinal surfaces are the same (= 25 nm). It follows that the total areas on the hillsides of the step bunches for the (6 7 1) and (13 9 0) surfaces are ~2.5 times as large as those for the (17 18 1) and (15 13 0) surfaces, while the number of the step edges, namely, the step density, on each of the four vicinal surfaces is almost the same. We believe that the top edge of a step bunch has different electronic properties from its hillside as the electrons at the top edge are more isolated from other electrons and nuclei than those on the hillside, and would feel less electron–electron or electron–nucleus interactions. By taking advantage of the difference between the 4° off-oriented and 10° off-oriented samples, we can analyze the electronic properties of the top edges and hillsides of step bunches separately (see Sec. III C 2).

The result of the RHEED measurement for the (011) surface is shown in Fig. 6. The bulk terminated (011)-(1×1) structure is known to have a unit cell with 0.459 nm along

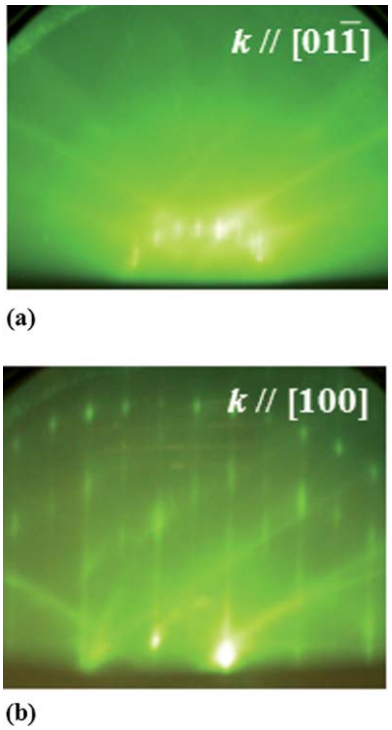

FIG. 6. RHEED patterns of TiO_2 (011). *k* vectors of electron beams were set parallel to (a) [0 1 $\bar{1}$] and (b) [1 0 0].

[1 0 0] and 0.545 nm along [0 $\bar{1}$ 1].[22] The RHEED measurement shows that the lengths of the unit cell along [1 0 0] and [0 1 $\bar{1}$] are 0.92 and 0.54 nm, respectively. Thus, the (011) surface has a 2 × 1 reconstructed surface structure as observed in a number of other reports.[21–30] The (110) surface and four vicinal surfaces are expected to have (110)-(1×1) terraces since they went through the same surface treatment as was performed in our previous study.[14]

B. Photocatalytic activity measurement

The result of the TiO_2 photocatalytic activity measurement for the TiO_2 (110), (011), (17 18 1), and (15 13 0) surfaces is shown in Fig. 7. As shown in Fig. 7(a), a methylene blue aqueous solution has an absorption peak around 660 nm. After three-hour UV irradiation onto the TiO_2 (011) surface, the absorption peak clearly shrank. This means that methylene blue molecules were decomposed through a TiO_2 photodegradation reaction. In Fig. 7(b), concentration of a methylene blue aqueous solution estimated by transmittance at 660 nm is plotted as a function of UV illumination time. Concentration at an arbitrary time $C(t)$ is expressed as

$$C(t) = C_0 \frac{\ln T(t)}{\ln T_0}, \tag{1}$$

where $C_0 = C(0)$ is the initial concentration, $T_0 = T(0)$ is the initial transmittance, and $T(t)$ is the transmittance at an arbitrary time.

From Fig. 7(b), one can see that upon UV irradiation, each TiO_2 sample starts to decompose methylene blue molecules at a different rate. Each data set fit very well to an

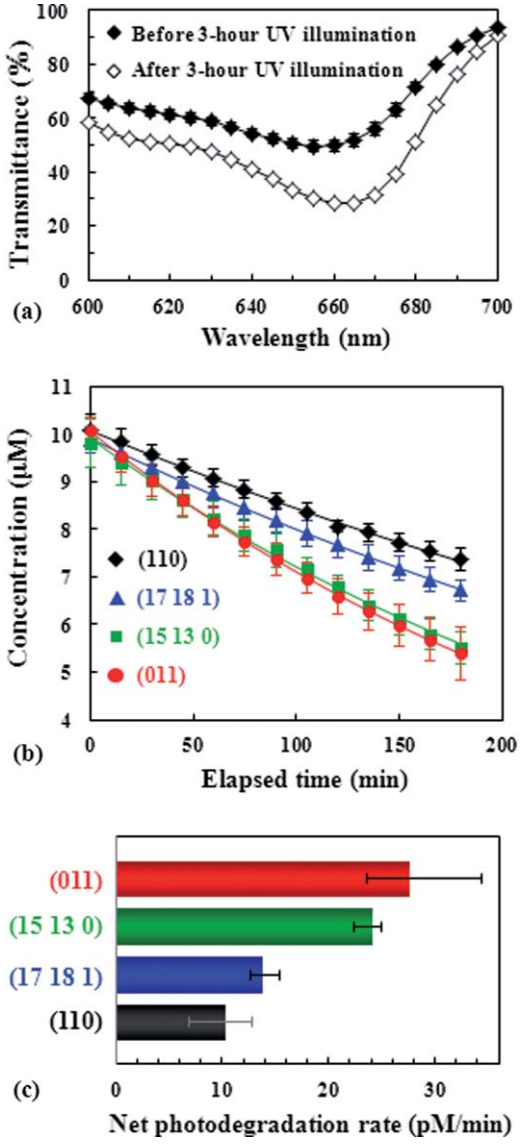

FIG. 7. (a) Transmission spectra of a methylene blue aqueous solution before and after three-hour UV illumination on TiO_2 (011). (b) Changes in the concentration of methylene blue molecules as a function of UV irradiation time for each sample. Each data set was fitted with an exponential decay curve to estimate a photodegradation rate. (c) Net photodegradation rates were estimated through the exponential fitting in (b).

exponential decay curve,

$$C(t) = C_0 \exp\left[-\frac{t}{\tau}\right], \tag{2}$$

and the photodegradation rate, $u = C_0/\tau$, was estimated through the fitted parameters. Note that a small number of methylene blue molecules were decomposed by UV irradiation even without TiO_2. The degradation rate without TiO_2, or u', was subtracted from the photodegradation rate u to obtain the net photodegradation rate, $v = u - u'$. The net photodegradation rate v for each sample is shown in Fig. 7(c).

Figure 7(c) shows that the (011) surface has a lot higher photocatalytic activity than the (110) surface. This result is in good agreement with the result reported by Yamamoto *et al.*[20] It is important to note that the TiO_2 (011) sample prepared by Yamamoto *et al.* went through a surface treatment procedure

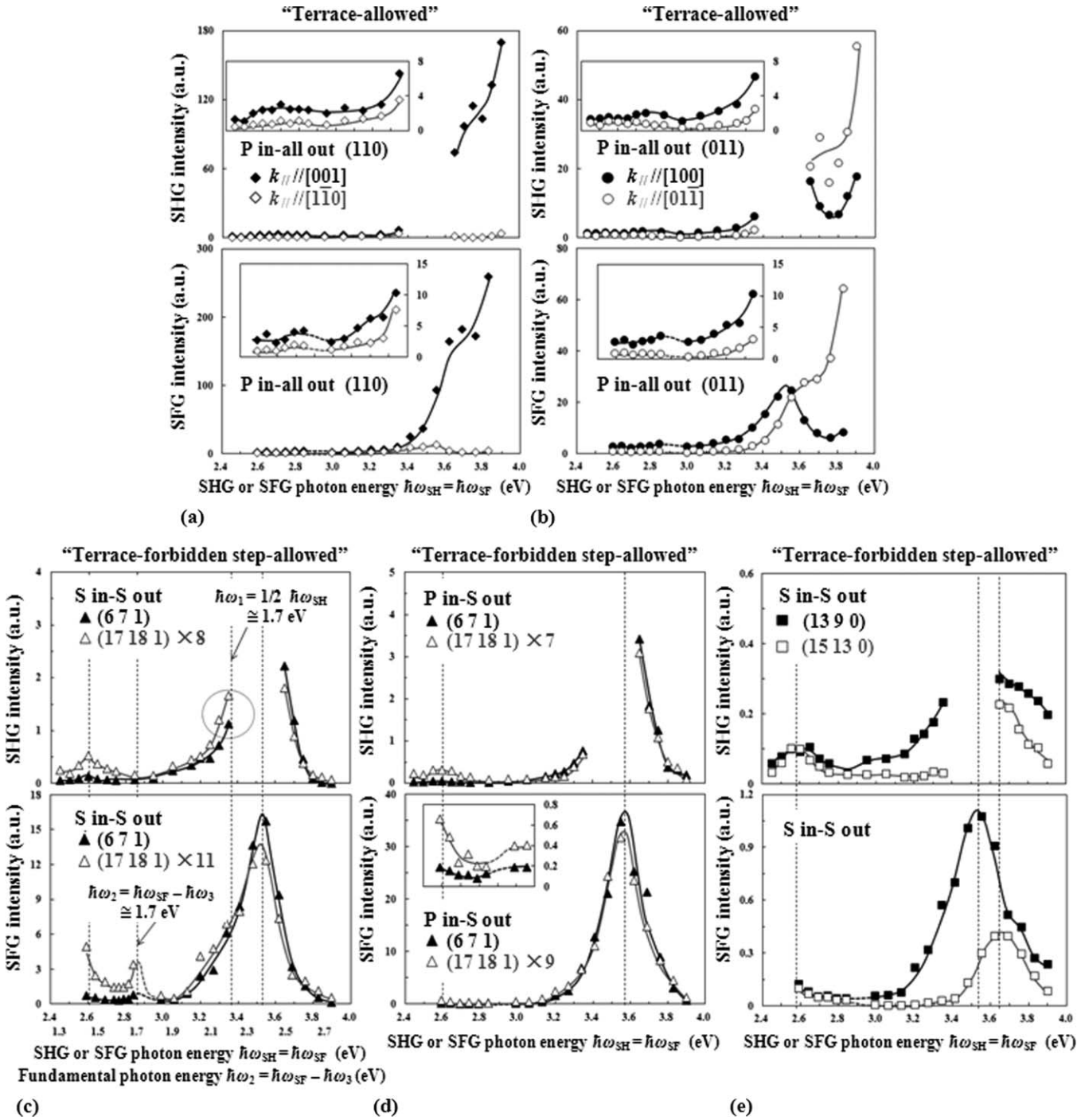

FIG. 8. SHG and SFG spectra of (a) TiO_2 (110) at P in-all out, (b) TiO_2 (011) at P in-all out, (c) TiO_2 (6 7 1) and (17 18 1) at S in-S out, (d) TiO_2 (6 7 1) and (17 18 1) at P in-S out, and (e) TiO_2 (13 9 0) and (15 13 0) at S in-S out. Incident angles of fundamental beams were set to ∼45° for (a) and (b), and were set to ∼2° for (c), (d), and (e). Directions of the incident planes are shown in Fig. 3.

similar to ours. However, Quah *et al*. suggested that the TiO_2 (011) surface treated in their ultrahigh vacuum (UHV) chamber probably possessed the recently proposed brookite (001)-like structure and did not exhibit any particular photocatalytic activity when compared to other rutile crystal faces.[30] We believe that the (011) surfaces prepared by us and Yamamoto *et al*. do not necessarily have the brookite (001)-like structure because the surface treatments done in our study and their study are totally different from the ones that have been done in other reports listed in the Refs. 21–30. Therefore, the notable reactivity of the (011) surface is not necessarily caused by the recently proposed brookite (001)-like structure.

The (17 18 1) and (15 13 0) surfaces, the vicinal surfaces of (110), showed higher photocatalytic activity than the (110) surface, indicating that the presence of the step bunches contributes to the enhancement of photocatalytic activity in some way. More interestingly, the (15 13 0) surface showed distinctly higher photocatalytic activity than the (17 18 1) surface within the range of error. This result suggests that TiO_2 photocatalytic activity depends on the direction of steps: steps

along [0 0 1] are more reactive than steps along [1 $\bar{1}$ 1]. It is important to remark that this is the first evaluation of TiO_2 photocatalytic activity among the flat and stepped surfaces.

C. SHG/SFG spectroscopy

1. Local electronic structures of the flat and stepped TiO_2 samples

The result of the SHG/SFG spectroscopy is shown in Fig. 8. The upper spectra correspond to the SHG spectra, and the lower spectra correspond to the SFG spectra. The SHG and SFG spectra have a common horizontal axis corresponding to SHG photon energy $\hbar\omega_{SH}$ or SFG photon energy $\hbar\omega_{SF}$ ($\hbar\omega_{SH} = \hbar\omega_{SF}$), and the axis labels are shown just below the horizontal axis. We also added another axis label corresponding to the fundamental photon energy $\hbar\omega_2 = \hbar\omega_{SF} - \hbar\omega_3$, where $\hbar\omega_3 = 1.17$ eV, right below the axis label of $\hbar\omega_{SH} = \hbar\omega_{SF}$ in Fig. 8(c) in order to discuss one-photon resonances in the SFG spectra. The solid and broken curves on the spectra are guide lines.

Remember that the SHG/SFG spectra for the TiO_2 vicinal surfaces shown in Figs. 8(c)–8(e) originate only from their step atoms and give us the information on their LDOS as a form of their valence-conduction band JDOS.[13] When an incident angle is increased near 45°, SHG and SFG come from the entire TiO_2 surface [Figs. 8(a) and 8(b)]. Since incident beams are almost normal to the (6 7 1) and (17 18 1) surfaces and satisfy $\vec{k}_{///}$//[1 $\bar{1}$ 0], as shown in Fig. 3(c), both the electric fields of incident beams and SHG/SFG beams are almost parallel to [0 0 1] in the case of S in-S out. Therefore, the SHG/SFG intensity I in Fig. 8(c) is roughly expressed by $I \propto |\chi^{(2)}_{xxx}|^2$ using second order nonlinear susceptibility elements $\chi^{(2)}_{ijk}$, where x is the [0 0 1] direction and y is the [1 $\bar{1}$ 0] direction. For P in-S out, the electric fields of incident beams are almost parallel to y, and thus the SHG/SFG intensity in Fig. 8(d) is roughly expressed by $I \propto |\chi^{(2)}_{xyy}|^2$. Similarly, the SHG/SFG intensity in Fig. 8(e) can be described as $I \propto |\chi^{(2)}_{yyy}|^2$. These second order nonlinear susceptibility elements are well discussed in Ref. 14.

In Fig. 8, strong SHG/SFG responses were observed for all the samples at SHG/SFG photon energies above the band-gap energy of rutile TiO_2 (3.05 eV). These strong signals are attributed to two-photon resonances, as the SHG and SFG spectra for each sample show almost the same behavior at the same SHG/SFG photon energy range. These two-photon resonances are derived from valence-conduction interband electronic transitions. The two-photon resonances from the terraces on the flat (110) and (011) surfaces are almost 1 to 2 orders of magnitude stronger than those from the step bunches on the vicinal surfaces [Figs. 8(a) and 8(b)]. Peak structures at ~3.55 eV characterized especially by the SHG/SFG spectra of the vicinal surfaces [Figs. 8(c)–8(e)] suggest that the LDOS at the step bunches of the vicinal surfaces is primarily distributed right below the valence band maximums (VBM) and right above the conduction band minimum (CBM) as depicted in Figs. 9(b) and 9(c).

Even though the (110) and (011) surfaces have totally different surface structures and different photocatalytic activity

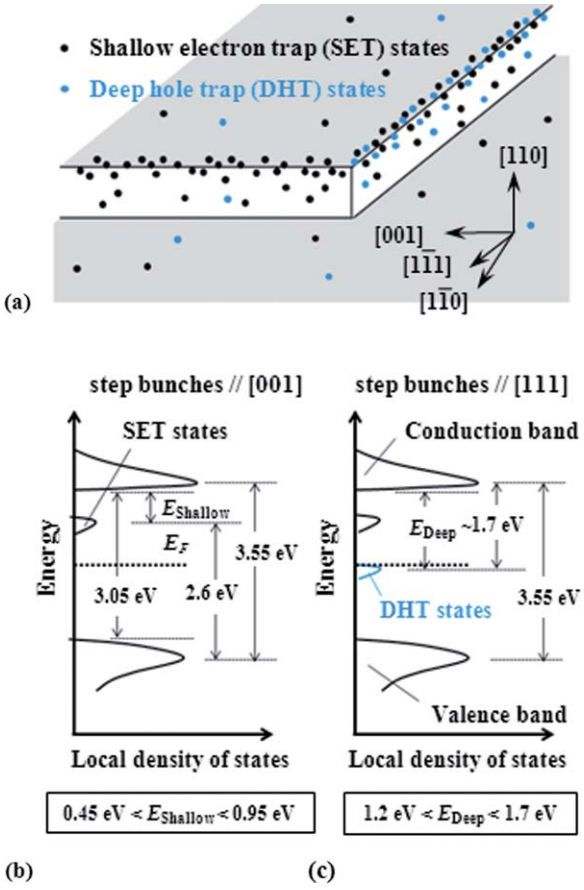

FIG. 9. Summary of the DHT and SET states observed by SHG/SFG spectroscopy. (a) Spatial distribution of the trap states on TiO_2 (110). (b), (c) Local density of states (LDOS) expected for the step bunches // [0 0 1] and // [1 $\bar{1}$ 1], respectively. The dashed lines in the center of the band gap in (b) and (c) corresponds to the Fermi level (E_F).

as shown in Figs. 7(b) and 7(c), their SHG/SFG spectra look quite similar, indicating that the surface band structures of the (110) and (011) surfaces are quite similar to each other. This tendency is analogous to the result of density of states (DOS) calculation for TiO_2 (110) and (011) conducted by Beck *et al.* using a titanyl (Ti = O) model as a (011)-(2×1) reconstructed structure.[21] However, their DOS calculation displayed one interesting difference between (110) and (011) at their VBM. That is, localized states associated with one-fold O atoms, which can act as efficient hole trapping sites and facilitate photo-oxidation reactions, were found only at the VBM of TiO_2 (011). Similarly, one can see one obvious difference between the SHG/SFG spectra of the (110) and (011) surfaces: for the (110) surface, the SHG/SFG intensity of the spectrum for Fig. 8(a) ◊ is much smaller than that of the another one [Fig. 8(a) ◆] above the SHG/SFG photon energy of 3.4 eV, whereas there is no remarkable difference in the SHG/SFG intensity between the two spectra of the (011) surface in the whole photon energy range [Fig. 8(b) • and ○]. Analogous to the result of the DOS calculation, the pronounced SHG/SFG response for Fig. 8(b) • around 3.5 eV compared to Fig. 8(a) ◊ implies the presence of some intrinsic surface electronic states around the VBM (or possibly around the CBM) of the (011) surface. As suggested by Beck *et al.*, it is inferred that the

TABLE II. Summary of the spectroscopic information on the step bunches and terraces. The step bunches //[1 $\bar{1}$ 1] correspond to the step bunches formed on the (6 7 1) and (17 18 1) surfaces, and the step bunches //[0 0 1] correspond to the step bunches formed on the (13 9 0) and (15 13 0) surfaces. The parentheses in the columns of DHT states and SET states mean that the corresponding structures are not the primary sources of the resonances.

Structures	Energy ranges of SHG/SFG responses (peak positions)	DHT states	SET states
(110) terraces	$k_{////}$[0 0 1] : > 3.4 eV $k_{////}$[1 $\bar{1}$ 0] : $3.4 - 3.6$ eV(~ 3.55 eV)	Not found	Structureless weak resonance
(011) terraces	$k_{////}$[1 0 0] : $3.55 - 3.7$ eV(~ 3.55 eV) $k_{////}$[0 1 $\bar{1}$] : > 3.4 eV	Not found	Structureless weak resonance
Top edges of the step bunches // [1 $\bar{1}$ 1]	...	Resonant at $\sim$1.7 eV	Resonant at $\sim$2.6 eV
Hillsides of the step bunches // [1 $\bar{1}$ 1]	3.2−3.8 eV ($\sim$3.55 eV)	(Resonant at $\sim$1.7 eV)	(Resonant at $\sim$2.6 eV)
Top edges of the step bunches // [0 0 1]	3.5−3.9 eV ($\sim$3.65 eV)	Not found	Resonant at $\sim$2.6 eV
Hillsides of the step bunches // [0 0 1]	3.2−3.8 eV ($\sim$3.55 eV)	Not found	(Resonant at $\sim$2.6 eV)

presence of these electronic states on the (011) surface could contribute to enhancing its photocatalytic activity by precipitating molecular adsorption or interfacial charge transfers of holes (or electrons). Even though the titanyl (Ti = O) model seems slightly out of date now, it can give us a good insight. However, further analysis of these intrinsic electronic states would be required to understand their detailed properties and the reactivity of the (110) surface.

Another experimental fact that should be noted about the SHG/SFG spectra for the (110) and (011) surfaces is that any significant resonances from trap states were not observed for either the (110) or (011) surfaces below the band-gap energy of rutile TiO_2 as far as our scanning range of SHG/SFG photon energy is concerned. This does not necessarily mean that there are no trap states on the flat (110) and (011) surfaces because SHG/SFG intensity has nonzero values at SHG/SFG photon energies below the band-gap energy. The result of the SHG/SFG spectra for the (110) and (011) surfaces is summarized in Table II.

In contrast to the flat surfaces, we could observe remarkable resonances from trap states at 2.6 eV for both kinds of stepped surfaces [Figs. 8(c)–8(e)]. This result suggests that the trap states are more favorably formed at step bunches than on flat terraces, and that step structures may be primarily responsible for the formation of these trap states. These resonances are attributed to two-photon resonances, as the resonances from the shallow trap states could be seen in the same SHG/SFG photon energy range when compared between the SHG and SFG spectra. Since the feature of the resonances did not depend on the direction of the step bunches, the shallow trap states at the step bunches // [1 $\bar{1}$ 1] and // [0 0 1] should come from common defect sites, and thus are not affected by surrounding surface structures. We assigned the shallow trap states to Ti3d defect states, well-known electron trap states, associated with surface/subsurface oxygen vacancies[37–46] or near-surface titanium interstitials.[47–49] Therefore, the SHG/SFG resonances at 2.6 eV can be attributed to the electronic transition from the valence band to the unoccupied SET states [Figs. 9(b) and 9(c)] because the SHG/SFG intensity becomes high only when the initial and final states in the SHG/SFG process are electron-occupied and electron-unoccupied states, respectively. In Fig. 9, we assume that the Fermi level (E_F) is located in the center of the band gap since our samples are well oxidized during the process of the annealing in an O_2 gas and should act as intrinsic semiconductors. Note that the value of the SHG/SFG resonant energy, 2.6 eV, does not necessarily mean that the center of the SET states is located exactly 2.6 eV above the VBM (or 0.45 eV below the CBM). As shown in Figs. 9(b) and 9(c), the center of the SET states should be located between 0.45 and 0.95 eV below the CBM because the SHG/SFG spectra reflect TiO_2 valence-conduction band JDOS. In the literature, these Ti3d defect states were found to be located 0.7–1.0 eV below E_F in UPS.[38,45–47,75] In this case, it can be assumed that E_F is located almost at the edge of the conduction band as the samples used in UPS are reduced sufficiently by ion sputtering and vacuum annealing. Therefore, the energy levels of the Ti3d defect states observed in this study are in approximate agreement with the literature.

If surface oxygen vacancies are present at the step bunches, some of them are expected to be healed by oxygen molecules in air,[76–79] and the others ought to be hydroxylated to form Ti−OH groups during the process of our surface treatment due to the strong dissociative adsorption of water molecules at surface oxygen vacancy sites.[75,80–84] The electronic properties of surface oxygen vacancies (Ti^{3+} defects) are believed to remain unchanged even after the water dissociative adsorption at these sites[85] and the resultant Ti−OH groups behave as good electron trapping sites.[39,85] The presence of the electron trapping sites (Ti3d defect sites), including Ti−OH groups, at the step bunches should play an important role in photocatalytic reactions since they can serve as a tunnel for O_2 molecules to scavenge electrons. As mentioned earlier, the electron scavenging process by O_2 molecules is very important because it provides the pathway to produce well-known oxidizing agents, such as $O_2^{\bullet -}$, H_2O_2, and $^1O_2$,[3,32,50–52] as well as it prevents the recombination of holes.[53–55] Therefore, we believe that the presence of the SET states at the step bunches are partially responsible for the high photocatalytic activity of the vicinal surfaces compared to the flat (110) surface [Figs. 7(b) and 7(c)]. Another possible cause of the relatively high reactivity of the vicinal surfaces is the strong adsorption of reacting molecules at the step

bunches, as the Ti3d defect sites at the step bunches can facilitate the adsorption of not only water or oxygen molecules but also of reacting molecules, such as methylene blue. Adsorption of reacting molecules is very important since one of the important factors in catalytic reactions is how long the reacting molecules stay on a catalyst surface if we assume a Langmuir–Hinshelwood model.[86] However, we cannot tell only from the results of SHG/SFG spectroscopy whether the step bunches really contribute to the strong adsorption of reacting molecules. This would be one of our future studies.

In addition to the resonances at 2.6 eV, we observed another resonance at $\hbar\omega_{SF} \cong 2.85$ eV in the SFG spectra of the (6 7 1) and (17 18 1) surfaces at S in-S out [the lower spectra of Fig. 8(c)]. We can attribute this resonance to a one-photon resonance at $\hbar\omega_2 \cong 1.7$ eV, not a two-photon resonance at $\hbar\omega_{SF} \cong 2.85$ eV, as the corresponding SHG spectra [the upper spectra of Fig. 8(c)] did not show any remarkable resonances at $\hbar\omega_{SH} \cong 2.85$ eV. If there is really a one-photon resonance at ~1.7 eV, the resonance should also be observed at $\hbar\omega_{SH} \cong 3.4$ eV in the SHG spectra as indicated in the upper spectra of Fig. 8(c). Due to the strong two-photon resonances in this range, however, a one-photon resonance cannot be observed in the SHG spectra clearly as compared to the SFG spectra. We discuss the one-photon resonance in the SHG spectra in detail later. It is important to remark that the one-photon resonance was intrinsic to the step bunches // [1 $\bar{1}$ 1], and was not observed at P in-S out but at S in-S out. This result indicates that the one-photon resonance at ~1.7 eV occurs only when $\chi^{(2)}_{xxx}$ (not $\chi^{(2)}_{xyy}$) is involved in the nonlinear optical process.

We believe that the origin of the one-photon resonance at ~1.7 eV is identical to that of the PL at ~840 nm detected by other groups.[42,57–62] The one-photon resonance is therefore attributed to the electronic transition from the occupied DHT states to the conduction band. Excited DHT states (electron-unoccupied states) may be localized at some oxygen atoms at the TiO_2 surface or subsurface as mentioned in the Introduction. Our result adds more information to the results reported by other groups: the formation of the DHT states requires or is facilitated by some special lattice coordination as is present at the step bunches // [1 $\bar{1}$ 1]. However, it is difficult to identify the lattice coordination in question because of the complex structures of the step bunches. From the similar discussion as was given for the SET states, the center of the deep hole levels is not located exactly 1.7 eV below the CBM, and the DHT states should be located between 1.2 and 1.7 eV below the CBM, namely, near the center of the band gap [Fig. 9(c)]. Therefore, the corresponding energy of the DHT states is in good agreement with the one estimated through PL.[42,57–62] Spatial distribution of the DHT and SET states on a TiO_2 surface and their energy levels are summarized in Fig. 9.

Now, we discuss the relationship between the presence of the DHT states and the photocatalytic activity. Remember that the (17 18 1) surface showed the lower photocatalytic activity than the (15 13 0) surface did [Figs. 6(b) and 6(c)], and that the (15 13 0) surface did not exhibit any resonances from DHT states [Fig. 8(e)]. According to the idea given by Bahnemann *et al.*,[33] these results indicate that the presence of the DHT states observed from the step bunches // [1 $\bar{1}$ 1] did not effectively contribute to the decomposition of methylene blue molecules. One possible reason for this is that the $^{\bullet}$OH radical production from the DHT states or the reaction between methylene blue molecules and surface-bound hydroxyl radicals (Ti−$^{\bullet}$OH) produced from deeply trapped holes was so slow that the presence of the DHT states could not enhance the reactivity of the (17 18 1) surface. As a matter of fact, the $^{\bullet}$OH radical production rate for the rutile phase is reported to be considerably slower than that for the anatase phase.[87] This slow $^{\bullet}$OH radical production could even deteriorate the photocatalytic activity of the (17 18 1) surface since it may result in promoting the recombination at the DHT sites, and thus this can be one of the reasons why the reactivity of the (17 18 1) surface did not stand out well among the vicinal surfaces.

2. Detailed analysis of SHG/SFG responses from the step bunches

SHG and SFG from the top edges of step bunches are more important than those from their hillsides because the less-coordinated structures at the top edges can give rise to anomalous electronic properties modifying photocatalytic reactions. Therefore, it is important to analyze the SHG/SFG spectra for the vicinal surfaces in detail. By comparing the SHG/SFG signals between the 4° off-oriented and 10° off-oriented samples, we can analyze electronic properties of the top edges and hillsides of step bunches separately. Remember that the total areas on the hillsides of the step bunches for the 10° off-oriented (6 7 1) and (13 9 0) surfaces are estimated to be ~2.5 times as large as those for the 4° off-oriented (17 18 1) and (15 13 0) surfaces, while the number of the step edges on each of the four vicinal surfaces is almost the same. Under this assumption, contributions to the total SHG/SFG from the hillside component should be much smaller for the (17 18 1) and (15 13 0) surfaces than for the (6 7 1) and (13 9 0) surfaces. In contrast, contributions from the top edge component for the 4° off-oriented and 10° off-oriented samples are expected to be comparable to each other. It follows that the effect from the top edge component should be more emphasized in the SHG/SFG spectra of the (17 18 1) and (15 13 0) surfaces than those of the (6 7 1) and (13 9 0) surfaces, although the (17 18 1) and (15 13 0) surfaces give lower SHG/SFG intensity in total.

For the (6 7 1) and (17 18 1) surfaces, the peak intensity at 3.55 eV for the (17 18 1) surface was almost 10 times smaller than that for the (6 7 1) surface [Figs. 8(c) and 8(d)]. Note that the SHG/SFG spectra of the (17 18 1) surface are magnified to compare the peak shapes. We conclude that these peaks at 3.55 eV derive primarily from the hillsides of the step bunches since the peak intensity strongly depended on the miscut angles of the samples. In contrast to the peaks at 3.55 eV, the resonances at 2.6 and ~1.7 eV did not show significant differences in the SHG/SFG intensity between the (6 7 1) and (17 18 1) surfaces, and stood out more in the spectra of the (17 18 1) surface than those of the (6 7 1) surface. The same tendency was observed for the resonance at 2.6 eV in the SHG/SFG spectra of the (13 9 0) and (15 13 0) surfaces

[Fig. 8(e)]. These results suggest that the DHT and SET states primarily arise from the top edges of the step bunches rather than on their hillside.

A close inspection of peak shapes at 3.55 eV between the (6 7 1) and (17 18 1) surfaces shows that though they are equivalent for P in-S out [Fig. 8(d)], there is a slight difference in their peak shapes around 3.35 eV in the SHG spectra for S in-S out as indicated by a circle [the upper spectra of Fig. 8(c)]. This difference may be caused by the one-photon resonance at $\hbar\omega_1 = \hbar\omega_{SH}/2 \cong 1.7$ eV. As discussed above, the one-photon resonance from the DHT states derives from the top edge component. If so, the effect from the one-photon resonance at $\hbar\omega_1 = \hbar\omega_{SH}/2 \cong 1.7$ eV should be more pronounced in the SHG spectra of the (17 18 1) surface than those of the (6 7 1) surface and causes some differences in their peak shape. If the one-photon resonance is driven by the hillside component, there should be no difference in their peak shape. This result supports that the one-photon resonance from the DHT states is located around 1.7 eV and comes mainly from the top edges of the step bunches.

In the same manner, we conducted peak assignments for the (13 9 0) and (15 13 0) surfaces as well [Fig. 8(e)]. The peak at 3.55 eV in the spectra of the (13 9 0) surface is assigned to the effect from the hillside component. Furthermore, we assigned the shoulder observed from the (13 9 0) surface and the peak at 3.65 eV observed from the (15 13 0) surface to the effect from the top edge component since their intensity did not strongly depend on the miscut angles of the samples. The effect from the hillside component for the (15 13 0) surface may be so small that it is completely hidden under the tail of the peak at 3.65 eV. Based on these peak assignments, it is concluded that the SHG/SFG response energies for the top edges of the step bunches // [0 0 1] are higher than those for their hillside, indicating that there should be obvious differences in their LDOS distribution near the band-gap regions.

We summarize the above discussion on the SHG/SFG responses from the step bunches in Table II. We did not see any effects from the top edge component above 3.05 eV for the step bunches // [1 $\bar{1}$ 1], whereas we observed the effect from both the top edge and hillside components for the step bunches // [0 0 1]. The SHG/SFG intensity for the (6 7 1) surface is almost 10 times as strong at 3.55 eV as that for the (13 9 0) surface [Fig. 8(c)–8(e)]. This means that the effect from the hillside component is very strong for the step bunches // [1 $\bar{1}$ 1] compared to the step bunches // [0 0 1] that it could hide the effect from the top edge component of the step bunches // [1 $\bar{1}$ 1]. Another tentative interpretation is that the effect from the top edge component of the step bunches // [1 $\bar{1}$ 1] just overlapped with that from the hillside component in the same photon energy region. As far as trap states are concerned, the SHG/SFG signals were found to come from the top edge of the step bunches rather than their hillside for both kinds of step bunches.

D. DFT model calculation of LDOS

For the step bunches // [0 0 1], the SHG/SFG response energies were clearly different between the top edges and hillsides of the step bunches (Table II), indicative of a significant difference in their LDOS distribution near the gap regions. This difference in their local electronic structures is very interesting in terms of catalytic chemistry as well as surface physics because it is possible that this difference could be correlated with the outstanding reactivity of the (15 13 0) surface as compared to the (17 18 1) surface [Figs. 7(b) and 7(c)]. Thus, we calculated the LDOS on the TiO_2 (5 2 0) vicinal surface with a step parallel to [0 0 1] using DFT in order to figure out how the valence and/or conduction bands of the step bunches are modulated when compared to those of the terraces and bulk.

The slab model used in the DFT calculation is shown in Fig. 10(a). We built up the slab model based on the result of the AFM measurement for the (15 13 0) surface in Fig. 4(d).

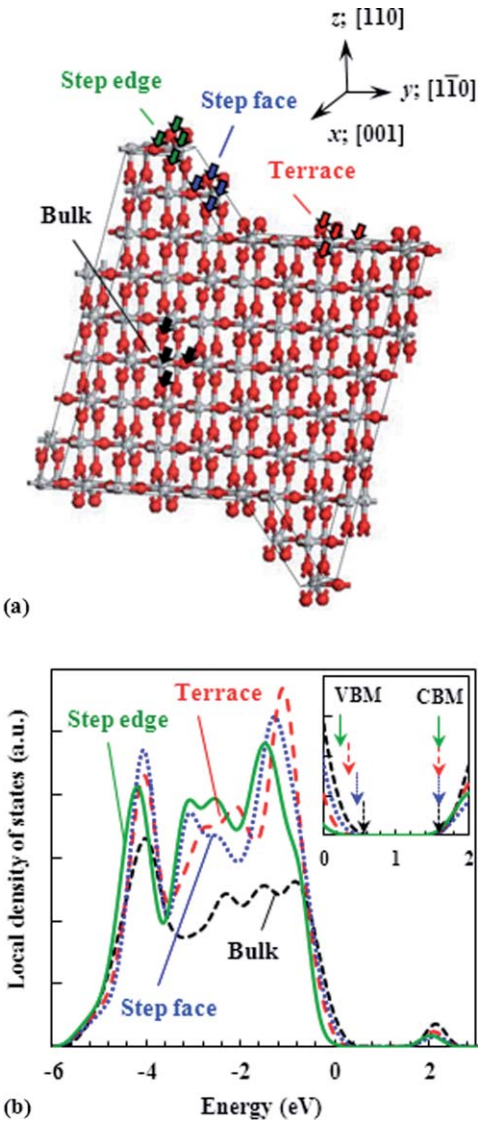

FIG. 10. (a) A rutile TiO_2 slab model for the DFT calculation of the LDOS. The surface of the slab model consists of a (110) terrace and a double-layer step parallel to [0 0 1] with a (100) step face. (b) Calculated LDOS for bulk, a terrace, a step face, and a step edge. For each structure, the LDOS at the four atoms indicated by the arrows in (a) is summed up to yield the total LDOS at the structure. The inset in (b) is the magnified scale of the LDOS near the band-gap region. VBM and CBM for each structure are indicated by the arrows in the inset. Energy zero corresponds to the Fermi energy.

As already discussed, we found that the (15 13 0) surface is made up of the multilayer step bunches (≥2 ML) and the (110) terraces with a terrace width of about 20–25 nm along [1 $\bar{1}$ 0]. However, since the size of the model system is limited, we assumed that the surface was composed of a bilayer step with a (100) step face, and a (110) terrace with a terrace width of four unit cells (2.6 nm) along [1 $\bar{1}$ 0]. Thickness of the slab was nine layers. The atomic structure at the step edge was referred to the model suggested by Diebold *et al.*[31] (Fig. 5).

The LDOS was calculated for bulk, a terrace, a step face, and a step edge [Fig. 10(b)]. The LDOS for each structure was made up of the LDOS of three inhomogeneous oxygen atoms and one titanium atom [Fig. 10(a)]. One can see that the LDOS around the VBM for the step and the terrace is shifted from the corresponding LDOS for the bulk to lower energy, whereas the CBM for each of these four structures remains almost at the same energy. This tendency is also seen in the result of the theoretical calculation performed by Sano *et al.* that the DOS near the VBM for a (110) face undergoes a lower energy shift due to surface relaxation.[88] The red shifts of the LDOS in Fig. 10(b) become increasingly more significant for the step face, the terraces, and the step edge. This is consistent with the result of the SHG/SFG spectroscopy. As summarized in Table II, the minimum of the SHG/SFG response energies for the top edges of the step bunches // [0 0 1] was higher than that for their hillsides and the (110) terraces. In other words, the band-gap energy for the top edges of the step bunches // [0 0 1] is larger than that for their hillsides and the (110) terraces. Therefore, it is concluded that the LDOS around the VBM for the top edges of the step bunches // [0 0 1] undergoes a red shift from the corresponding DOS for the bulk more significantly than that for their hillside and the (110) terraces does.

The red shift of the LDOS around the VBM for the top edges of the step bunches can give high oxidation power to free holes at these sites, as free holes extract electrons from adsorbed molecules more strongly with the increase in their potential energy (redox potential). However, we cannot tell at this stage whether these free holes really contribute to methylene blue photodegradation reactions or not. In this paper, we failed to completely explain the origin of the high reactivity of the step bunches, especially the ones // [0 0 1], as well as that of the (011) face in terms of trap states or LDOS near the band-gap regions. To make this problem clearer, we need to look into not only static surface electronic properties but also dynamic properties at TiO_2 surfaces after UV excitation.

IV. CONCLUSION

In this study, SHG/SFG spectroscopy, AFM, and photocatalytic activity measurements were performed for rutile TiO_2 (110)-(1×1), (011)-(2×1), (17 18 1), and (15 13 0). We attained selective measurement of the local electronic structures of the step bunches formed on the vicinal surfaces using a SHG/SFG step-selective probing technique. The surface electronic structures of the flat (110) (the terrace face of the vicinal surfaces) and (011) surfaces were also discussed. The SHG/SFG spectra for the (110) and (011) surfaces showed that their surface band structures look quite similar to each other, and also implied that only the (011) surface has some specific electronic states around the VBM (or possibly around the CBM). In addition, any significant resonances from trap states were not observed for these samples within the experimental limit of the SHG/SFG photon energy range. For the vicinal surfaces, on the other hand, we detected DHT and SET states selectively from the step bunches. This result suggests that the formation of the trap states is more likely to be precipitated at the step bunches than on the flat terraces. The energy levels of these DHT and SET states were estimated to be between 1.2 and 1.7 eV below the CBM and between 0.45 and 0.95 eV below the CBM, respectively, and are in approximate agreement with the literature. Unlike the SET states, the DHT states were observed only at the step bunches // [1 $\bar{1}$ 1]. This implies that the formation of the DHT states may require or be facilitated by some special lattice coordination as is present at the step bunches // [1 $\bar{1}$ 1]. Photocatalytic activity of each TiO_2 sample was found to follow the sequence: (110) < (17 18 1) < (15 13 0) < (011), indicating that steps // [0 0 1] are more reactive than steps // [1 $\bar{1}$ 1]. This result implies that the presence of the DHT states at the step bunches // [1 $\bar{1}$ 1] did not effectively contribute to the methylene blue photodegradation reactions.

Detailed analysis of the SHG/SFG spectra allowed us to distinguish the SHG/SFG signals between the top edge and hillside of the step bunches on the vicinal surfaces, and showed that the DHT and SET states prefer to be formed at their top edges rather than on their hillsides. The DFT calculation, in line with the SHG/SFG spectroscopy, suggests that the LDOS around the VBM for the top edges of the step bunches // [0 0 1] undergoes a red shift from the corresponding DOS for the bulk more significantly than that for their hillsides and the (110) terraces does. However, it still remains unclear whether this red shift of the LDOS for the top edges is really correlated with the outstanding reactivity of the (15 13 0) surface as compared to the (17 18 1) surface.

ACKNOWLEDGMENTS

The authors gratefully acknowledge Dr. A. Sasahara, Y. Nakabayashi, and M. Uno for experimental supports, and Dr. D. H. Chi and Professor K. Ebitani for valuable discussions. The authors wish to thank Dr. A. Steigerwald and Dr. H. Park for helpful advices.

[1] A. Fujishima, T. N. Rao, and D. A. Tryk, J. Photochem. Photobiol. C **1**, 1 (2000).
[2] U. Diebold, Surf. Sci. Rep. **48**, 53 (2003).
[3] A. Fujishima, X. Zhang, and D. A. Tryk, Surf. Sci. Rep. **63**, 515 (2008).
[4] T. F. Heinz, F. J. Himpsel, and E. Burstein, Phys. Rev. Lett. **63**, 644 (1989).
[5] A. N. Shultz, W. Jang, W. M. HetheringtonIII, D. R. Baer, Li.-Q. Wang, and J. H. Engelhard, Surf. Sci. **339**, 114 (1995).
[6] E. Kobayashi, T. Wakasugi, G. Mizutani, and S. Ushioda, Surf. Sci. **402**, 537 (1998).
[7] E. Kobayashi, K. Matsuda, G. Mizutani, and S. Ushioda, Surf. Sci. **427**, 294 (1999).
[8] M. Omote, H. Kitaoka, E. Kobayashi, O. Suzuki, K. Aratake, H. Sano, G. Mizutani, W. Wolf, and R. Podloucky, J. Phys.: Condens. Matter **17**, S175 (2005).
[9] G. Mizutani, J. Kameya, N. Ishibashi, S. Tanaka, T. Sekiya, and S. Kurita, Recent Res. Dev. Opt. **3**, 649 (2003).

[10]J. P. Fitts, M. L. Machesky, D. J. Wesolowski, X. Shang, J. D. Kubicki, G. W. Flynn, T. F. Heinz, and K. B. Eisenthal, Chem. Phys. Lett. **411**, 399 (2005).
[11]J. M. Lantz and R. M. Corn, J. Phys. Chem. **98**, 4899 (1994).
[12]J. M. Lantz and R. M. Corn, J. Phys. Chem. **98**, 9387 (1994).
[13]H. Takahashi, R. Watanabe, and G. Mizutani, Surf. Interface Anal. **42**, 1659 (2010).
[14]H. Takahashi, R. Watanabe, and G. Mizutani, e-J. Surf. Sci. Nanotechnol. **8**, 84 (2010).
[15]X.-Q. Gong and A. Selloni, J. Catal. **249**, 134 (2007).
[16]X.-Q. Gong, A. Selloni, M. Batzill, and U. Diebold, Nature Mater. **5**, 665 (2006).
[17]X.-Q. Gong, A. Selloni, O. Dulub, P. Jacobson, and U. Diebold, J. Am. Chem. Soc. **130**, 370 (2008).
[18]A. Sasahara, C. L. Pang, and H. Onishi, J. Phys. Chem. B **110**, 4751 (2006).
[19]J. E. Ortega, A. Mugarza, V. Repain, S. Rousset, V. Pérez-Dieste, and A. Mascaraque, Phys. Rev. B **65**, 165413 (2002).
[20]Y. Yamamoto, K. Nakajima, T. Ohsawa, Y. Matsumoto, and H. Koinuma, Jpn. J. Appl. Phys. **44**, L511 (2005).
[21]T. J. Beck, A. Klust, M. Batzill, U. Diebold, C. Di Valentin, and A. Selloni, Phys. Rev. Lett. **93**, 036104 (2004).
[22]O. Dulub, C. Di Valentin, A. Selloni, and U. Diebold, Surf. Sci. **600**, 4407 (2006).
[23]T. J. Beck, A. Klust, M. Batzill, U. Diebold, C. Di Valentin, A. Tilocca, and A. Selloni, Surf. Sci. **591**, L267 (2005).
[24]C. Di Valentin, A. Tilocca, A. Selloni, T. J. Beck, A. Klust, M. Batzill, Y. Losovij, and U. Diebold, J. Am. Chem. Soc. **127**, 9895 (2005).
[25]T. Kubo, H. Orita, and H. Nozoye, J. Am. Chem. Soc. **129**, 10474 (2007).
[26]X.-Q. Gong, N. Khorshidi, A. Stierle, V. Vonk, C. Ellinger, H. Dosch, H. Cheng, A. Selloni, Y. He, O. Dulub, and U. Diebold, Surf. Sci. **603**, 138 (2009).
[27]X. Torrelles, G. Cabailh, R. Lindsay, O. Bikondoa, J. Roy, J. Zegenhagen, G. Teobaldi, W. A. Hofer, and G. Thornton, Phys. Rev. Lett. **101**, 185501 (2008).
[28]S. E. Chamberlin, C. J. Hirschmugl, H. C. Poon, and D. K. Saldin, Surf. Sci. **603**, 3367 (2009).
[29]Y. He, W.-K. Li, X.-Q. Gong, O. Dulub, A. Selloni, and U. Diebold, J. Phys. Chem. C **113**, 10329 (2009).
[30]E. L. Quah, J. N. Wilson, and H. Idriss, Langmuir **26**, 6411 (2010).
[31]U. Diebold, J. Lehman, T. Mahmoud, M. Kuhn, G. Leonardelli, W. Hebenstreit, M. Schmid, and P. Varga, Surf. Sci. **411**, 137 (1998).
[32]M. R. Hoffmann, S. T. Martin, W. Choi, and D. W. Bahnemann, Chem. Rev. **95**, 69 (1995).
[33]D. W. Bahnemann, M. Hilgendorff, and R. Memming, J. Phys. Chem. B **101**, 4265 (1997).
[34]T. Yoshihara, R. Katoh, A. Furube, Y. Tamaki, M. Murai, K. Hara, S. Murata, H. Arakawa, and M. Tachiya, J. Phys. Chem. B **108**, 3817 (2004).
[35]Y. Tamaki, A. Furube, M. Murai, K. Hara, R. Katoh, and M. Tachiya, Phys. Chem. Chem. Phys. **9**, 1453 (2007).
[36]Y. Tamaki, K. Hara, R. Katoh, M. Tachiya, and A. Furube, J. Phys. Chem. C **113**, 11741 (2009).
[37]N. D. Abazović, M. I. Čomor, M. D. Dramićanin, D. J. Jovanović, S. P. Ahrenkiel, and J. M. Nedeljković, J. Phys. Chem. B **110**, 25366 (2006).
[38]C. M. Yim, C. L. Pang, and G. Thornton, Phys. Rev. Lett. **104**, 036806 (2010).
[39]C. Di Valentin, G. Pacchioni, and A. Selloni, Phys. Rev. Lett. **97**, 166803 (2006).
[40]M. Komiyama and Y. Li, Jpn. J. Appl. Phys. **43**, 4584 (2004).
[41]M. Komiyama and Y. Li, Appl. Surf. Sci. **244**, 550 (2005).
[42]A. K. Ghosh, F. G. Wakim, and R. R. Addiss, Phys. Rev. **184**, 979 (1969).
[43]S. Munnix and M. Schmeits, Phys. Rev. B **31**, 3369 (1985).
[44]F. M. Hossain, G. E. Muech, L. Sheppard, and J. Nowotny, Solid State Ionics **178**, 319 (2007).
[45]V. E. Henrich, G. Dresselhaus, and H. J. Zeiger, Phys. Rev. Lett. **36**, 1335 (1976).
[46]A. G. Thomas, W. R. Flavell, A. K. Mallick, A. R. Kumarasinghe, D. Tsoutsou, N. Khan, C. Chatwin, S. Rayner, G. C. Smith, R. L. Stockbauer, S. Warren, T. K. Johal, S. Patel, D. Holland, A. Taleb, and F. Wiame, Phys. Rev. B **75**, 035105 (2007).
[47]S. Wendt, P. T. Sprunger, E. Lira, G. K. H. Madsen, Z. Li, J. Ø. Hansen, J. Matthiesen, A. Blekinge-Rasmussen, E. Lægsgaard, B. Hammer, and F. Besenbacher, Science **320**, 1755 (2008).
[48]C. Di Valentin, G. Pacchioni, and A. Selloni, J. Phys. Chem. C **113**, 20543 (2009).
[49]E. Finazzi, C. Di Valentin, and G. Pacchioni, J. Phys. Chem. C **113**, 3382 (2009).
[50]Y. Nosaka, T. Daimon, A. Y. Nosaka, and Y. Murakami, Phys. Chem. Chem. Phys. **6**, 2917 (2004).
[51]T. Daimon and Y. Nosaka, J. Phys. Chem. C **111**, 4420 (2007).
[52]T. Hirakawa and Y. Nosaka, Langmuir **18**, 3247 (2002).
[53]T. Tan, D. Beydoun, and R. Amal, J. Photochem. Photobiol., A **159**, 273 (2003).
[54]N. K. Youn, J. E. Heo, O. S. Joo, H. Lee, J. Kim, and B. K. Min, J. Hazard. Mater. **177**, 216 (2010).
[55]D. Zhang, R. Qiu, L. Song, B. Eric, Y. Mo, and X. Huang, J. Hazard. Mater. **163**, 843 (2009).
[56]A. Sirisuk, E. Klansorn, and P. Praserthdam, Catal. Commun. **9**, 1810 (2008).
[57]Y. Nakato, A. Tsumura, and H. Tsubomura, J. Phys. Chem. **87**, 2402 (1983).
[58]Y. Nakato, H. Ogawa, K. Morita, and H. Tsubomura, J. Phys. Chem. **90**, 6210 (1986).
[59]R. Nakamura and Y. Nakato, J. Am. Chem. Soc. **126**, 1290 (2004).
[60]R. Nakamura, T. Okamura, N. Ohashi, A. Imanishi, and Y. Nakato, J. Am. Chem. Soc. **127**, 12975 (2005).
[61]A. Imanishi, T. Okamura, N. Ohashi, R. Nakamura, and Y. Nakato, J. Am. Chem. Soc. **129**, 11569 (2007).
[62]F. J. Knorr, C. C. Mercado, and J. L. McHale, J. Phys. Chem. C **112**, 12786 (2008).
[63]R. F. Howe and M. Grätzel, J. Phys. Chem. **91**, 3906 (1987).
[64]C. P. Kumar, N. O. Gopal, T. C. Wang, M.-S. Wong, and S. C. Ke, J. Phys. Chem. B **110**, 5223 (2006).
[65]N. O. Gopal, H.-H. Lo, S.-C. Sheu, and S.-C. Ke, J. Am. Chem. Soc. **132**, 10982 (2010).
[66]O. I. Micic, Y. Zhang, K. R. Cromack, A. D. Trifunac, and M. C. Thurnauer, J. Phys. Chem. **97**, 13284 (1993).
[67]O. I. Micic, Y. Zhang, K. R. Cromack, A. D. Trifunac, and M. C. Thurnauer, J. Phys. Chem. **97**, 7277 (1993).
[68]D. Lawless, N. Serpone, and D. Melsel, J. Phys. Chem. **95**, 5166 (1991).
[69]Y. Murakami, K. Endo, I. Ohta, A. Y. Nosaka, and Y. Nosaka, J. Phys. Chem. C **111**, 11339 (2007).
[70]Y. Maeda, T. Iwai, Y. Satake, K. Fujii, S. Miyatake, D. Miyazaki, and G. Mizutani, Phys. Rev. B **78**, 75440 (2008).
[71]B. Delley, J. Chem. Phys. **113**, 7756 (2000).
[72]H. Onishi and Y. Iwasawa, Surf. Sci. **313**, L783 (1994).
[73]V. Borovikov and A. Zangwill, Phys. Rev. B **79**, 245413 (2009).
[74]H. Hibino and T. Ogino, Phys. Rev. Lett. **72**, 657 (1994).
[75]R. L. Kurtz, R. Stockbauer, T. E. Madey, E. Román, and J. L. de Segovia, Surf. Sci. **218**, 178 (1989).
[76]Y. Du, Z. Dohnálek, and I. Lyubinetsky, J. Phys. Chem. C **112**, 2649 (2008).
[77]D. Sporleder, D. P. Wilson, and M. G. White, J. Phys. Chem. C **113**, 13180 (2009).
[78]S. Wendt, R. Schaub, J. Matthiesen, E. K. Vestergaard, E. Wahlström, M. D. Rasmussen, P. Thostrup, L. M. Molina, E. Lægsgaard, I. Stensgaard, B. Hammer, and F. Besenbacher, Surf. Sci. **598**, 226 (2005).
[79]E. Lira, J. Ø. Hansen, P. Huo, R. Bechstein, P. Galliker, E. Lægsgaard, B. Hammer, S. Wendt, and F. Besenbacher, Surf. Sci. **604**, 1945 (2010).
[80]Z. Zhang, B. Bondarchuk, B. D. Kay, J. M. White, and Z. Dohnalek, J. Phys. Chem. B **110**, 21840 (2006).
[81]I. M. Brookes, C. A. Muryn, and G. Thornton, Phys. Rev. Lett. **87**, 266103 (2001).
[82]Li.-M. Liu, P. Crawford, and P. Hu, Prog. Surf. Sci. **84**, 155 (2009).
[83]R. Schaub, P. Thostrup, N. Lopez, E. Lægsgaard, I. Stensgaard, J. K. Nørskov, and F. Besenbacher, Phys. Rev. Lett. **87**, 266104 (2001).
[84]S. Wendt, J. Matthiesen, R. Schaub, E. K. Vestergaard, E. Lægsgaard, F. Besenbacher, and B. Hammer, Phys. Rev. Lett. **96**, 066107 (2006).
[85]M. A. Henderson, W. S. Epling, C. H. F. Peden, and C. L. Perkins, J. Phys. Chem. B **107**, 534 (2003).
[86]T. M. El-Morsi, W. E. Budakowski, A. L. Abd-El-Aziz, and K. E. Friesen, Environ. Sci. Technol. **34**, 1018 (2000).
[87]T. Hirakawa, K. Yawata, and Y. Nosaka, Appl. Catal. A **325**,105 (2007).
[88]H. Sano and G. Mizutani, Phys. Rev. B **70**, 125411 (2004).